Protein Expression and Purification 133 (2017) 139–151

Contents lists available at ScienceDirect

Protein Expression and Purification

journal homepage: www.elsevier.com/locate/yprep

Optimized protocol for soluble prokaryotic expression, purification and structural analysis of human placenta specific-1(PLAC1)

Mahboobeh Nazari [a, b, *], Amir-hassan Zarnani [c, d], Roya Ghods [e, f], Rahman Emamzadeh [g], Somayeh Najafzadeh [h], Arash Minai-Tehrani [h], Jafar Mahmoudian [a, i], Maryam Yousefi [h], Sedigheh Vafaei [h], Sam Massahi [h], Mohammad-Reza Nejadmoghaddam [h, i]

[a] Monoclonal Antibody Research Center, Avicenna Research Institute, ACECR, Tehran, Iran
[b] Department of Tissue Engineering, School of Advanced Technologies in Medicine, Shahid Beheshti University of Medical Sciences, Tehran, Iran
[c] Department of Immunology, School of Public Health, Tehran University of Medical Sciences, Tehran, Iran
[d] Immunology Research Center, Iran University of Medical Sciences, Tehran, Iran
[e] Oncopathology Research Center, Iran University of Medical Sciences, Tehran, Iran
[f] Department of Molecular Medicine, Faculty of Advanced Technologies in Medicine, Iran University of Medical Sciences, IUMS, Tehran, Iran
[g] Department of Biology, Faculty of Sciences, University of Isfahan, Isfahan, Iran
[h] Nanobiotechnology Research Center, Avicenna Research Institute, ACECR, Tehran, Iran
[i] Nanotechnology Research Centre, Faculty of Pharmacy, Tehran University of Medical Sciences, Tehran, Iran

ARTICLE INFO

Article history:
Received 22 October 2016
Received in revised form
13 March 2017
Accepted 13 March 2017
Available online 16 March 2017

Keywords:
Placenta specific-1
Recombinant protein
Expression optimization
Soluble protein
Structure analysis

ABSTRACT

Placenta specific -1 (PLAC1) has been recently introduced as a small membrane-associated protein mainly involved in placental development. Expression of PLAC1 transcript has been documented in almost one hundred cancer cell lines standing for fourteen distinct cancer types. The presence of two disulfide bridges makes difficult to produce functional recombinant PLAC1 in soluble form with high yield. This limitation also complicates the structural studies of PLAC1, which is important for prediction of its physiological roles. To address this issue, we employed an expression matrix consisting of two expression vectors, five different *E. coli* hosts and five solubilization conditions to optimize production of full and truncated forms of human PLAC1. The recombinant proteins were then characterized using an anti-PLAC1-specific antibody in Western blotting (WB) and enzyme linked immunosorbent assay (ELISA). Structure of full length protein was also investigated using circular dichroism (CD). We demonstrated the combination of *Origami*™ and pCold expression vector to yield substantial amount of soluble truncated PLAC1 without further need for solubilization step. Full length PLAC1, however, expressed mostly as inclusion bodies with higher yield in *Origami*™ and *Rosetta2*. Among solubilization buffers examined, buffer containing Urea 2 M, pH 12 was found to be more effective. Recombinant proteins exhibited excellent reactivity as detected by ELISA and WB. The secondary structure of full length PLAC1 was considered by CD spectroscopy. Taken together, we introduced here a simple, affordable and efficient expression system for soluble PLAC1 production.

1. Introduction

Placenta-specific 1 (PLAC1) is a small (212 amino acid residues) membrane-associated protein [1] involved in placental development and its normal expression is almost restricted to placental trophoblast cells [2]. PLAC1-between different mammalian species - consists of (1)a conserved signal peptide from residues 1 to 23, (2) a number of well-conserved residues in transmembrane domain (TMD) (residues 20–50) and (3) an extremely conserved area in the extracellular space (residues 58–118) that is homologous to the N-terminal sub-domain of the zona pellucida (ZP3) glycoprotein [3,4]. PLAC1 is normally expressed in the apical villous surface of syncytiotrophoblasts and proposed to be involved in placenta anchoring to the endometrium that maintaining the contact during gestation [2]. Furthermore, the strong protein binding interaction was proposed to occur in ZP3-like extracellular domain [5].

The strong expression of PLAC1 was demonstrated in several

* Corresponding author.
E-mail addresses: Ma.nazari@ari.ir, nazari1980azar@yahoo.com (M. Nazari).

http://dx.doi.org/10.1016/j.pep.2017.03.011
1046-5928/

human solid tumors including; non small cell lung [6], breast [4], hepatocellular, colorectal [7,8], and gastric cancers [9], suggesting it has a role as an oncoplacental protein [10]. Recently, we observed that PLAC1 is differentially expressed in prostate cancer and has a strong positive association with Gleason score making it a potential protein target for immunotherapy of prostate cancer [11]. This molecule also was proposed as an attractive target for a set of cancers from histologically different origins [12].

Membrane proteins (MPs) are classified as the major set of protein drug targets due to their essential biological functions in the body [13–15]. Around 25% of all genes in both prokaryotes and eukaryotes including *PLAC1* encode for MPs [16]. Structural study and characterization of MPs call for an efficient expression systems yielding reasonable amount of protein in its native form. Cellular expression of recombinant membrane proteins, however, regularly outcomes in protein aggregation and misfolding that can be due to the hydrophobic properties of transmembrane parts. Expression of proteins at low levels or in insoluble form is considered a major challenging issue in structural biology [17]. In most instances, it is due to the inappropriate folding of human proteins in *Escherichia coli* cells, where they can be digested by proteases or accumulated as inclusion bodies (IBs) [17]. The poor protein expression has been demonstrated to be improved by gene manipulation [18,19]. On the other hand, the production of correctly-folded protein is reported to be more complicated and needs a balance between the rate of gene expression and the solubility of protein [20]. To improve proper protein folding and increase the yield of soluble protein, a variety of strategies have been established; 1) overproduction of recombinant proteins at low temperature; it has been reported that the temperature affects the rate of protein synthesis, folding kinetics [21,22] and the hydrophobic interactions involved in self aggregation as well as protein degradation [23]. Nonetheless, protein expression at low temperature can present some disadvantages, including reduced replication, transcription, and translation rates. These limitations have been proven to be avoided by using cold-inducible promoters such as cold shock promoter cspA [16–18] that optimize the rate of protein production at low temperature [24]. 2) Optimization of the cultivation conditions; the composition of the cell growth medium and the fermentation variables are important for the prevention of protein aggregation. A careful optimization has been shown to significantly improve the yield and quality of soluble protein production. 3) The expression of the protein of interest in fusion with recombinant tags such as thioredoxin (TRX) and glutathione-S-transferase (GST) [8–10]. Fusion partners are very stable peptide or protein molecules genetically connected to target proteins for optimization of the solubility and purification. 4) The use of *E. coli*-engineered host strains; introduction of DNA mutations in *E. coli* strains has been reported to alter protein synthesis, degradation, secretion, or folding [25]. The expression of proteins in oxidative cytoplasm of *Origami* or *Rosettagami* cells [26,27], where the formation of the disulfide bonds is more favored, improves folding of disulfide-containing proteins. And finally 5) Co-production of molecular chaperones and folding mediators [11]; the initial folding of proteins can be accompanied by molecular chaperones that avoid protein aggregation via binding to exposed hydrophobic areas on misfolded polypeptides, and transferring molecules to their specific sub-cellular target. Although, the expression of PLAC1 gene has been demonstrated in almost one hundred cancer cell lines standing for fourteen distinct cancers [4,6,7], its functional behavior remains unclear due to the lack of the structural information. Therefore, recombinant production of PLAC1 can be an attractive strategy to obtain large amounts of protein for further bioresearch applications. Here, we have demonstrated the expression of full length and truncated form of PLAC1 in *E. coli* and tried to optimize solubility of the recombinant protein using four out of five strategies mentioned above.

2. Materials and methods

2.1. Materials and strains

Following reagents and kits were used in this study. Isopropyl-ß-D-thiogalactopyranoside (IPTG), 3,3′,5,5′-Tetramethylbenzidine (TMB), phenylmethylsulfonyl fluoride (PMSF) and Ethylene diaminetetraacetic acid (EDTA), Guanidine hydrochloride (Gu.HCl) (Sigma-Aldrich, Germany), Ampicillin, T4 DNA ligase, shrimp alkaline phosphatase, restriction enzymes, M-MuLV Reverse transcriptase, Ellman's Reagent, DTNB(5,5'-dithio-bis-[2-nitrobenzoic acid]) (Thermo Scientific, USA), master mix 2× red (Ampliqon, Denmark), plasmid extraction kit, gel purification kit, polymerase chain reaction (PCR) purification kit (Qiagen, Germany), RNA isolation kit (CinnaGen, Iran), Ni sepharose high performance (GE healthcare, United Kingdom), enhanced chemiluminescence (ECL) Western Blotting Substrate (Pierce, Dalas, USA), pET-32a plasmid (Novagen, Germany), pColdI plasmid (Takara, Japan). Detailed information on strains of bacteria can be found in supporting information (SI) for materials and methods.

2.2. Extraction of total RNA

One gram of liquid nitrogen-frozen human placental tissue was pulverized under liquid nitrogen with a pestle. Total RNA was extracted using RNA isolation kit according to the manufacturer's instruction. Quality of purified RNA was analyzed by agarose gel electrophoresis and its concentration was determined by UV absorption spectroscopy at 260 nm.

2.3. Reverse transcriptase-PCR of PLAC1 gene

The first strand of cDNA was synthesized at 42 °C for 60 min in the presence of 200 U μl^{-1} M-MuLV Reverse transcriptase, 20 U RNase inhibitor, dNTP mix (final concentration each at 1 mM), and reverse primer. *PLAC1* (GenBank Accession No. NM_021796.3) transcript was then amplified using two pairs of specific primers designed for amplification of full length (*f-PLAC1*) (69–636) and truncated (*t-PLAC1*) (351–636) form. The sequences of primers for amplification of f-PLAC1 and t-PLAC1 were as follows: *f-PLAC1-S* 5′-AATTA***CATATG***CAAAGTCCAATGACTGTGCTGTG-3′ and *f-PLAC1-AS* 5′- ATAT***AAGCTT***TCACATGGACCCAATCATATCATC-3′, *t-PLAC1-S* 5′-AATTA***CATATG***GCCCCCCAAAAGTCCCCATG-3′ and the reverse primer was as the same with *f-PLAC1-AS*. *Nde*I and *Hind*III restriction sites (underlined bold sequences) were inserted in forward and reverse primers, respectively. The PCR amplification of cDNA was carried out using the first cDNA strand under the following condition: initial denaturation at 94 °C for 5 min, a 35- cycle amplification (94 °C for 1 min, 60 °C for 30 s, and 72 °C for 1 min), and a final extension for 5 min at 72 °C. Amplicons were digested by *Nde*I/*Hind*III and inserted into the *Nde*I/*Hind*III restriction sites of digested/dephosphorylated pColdI high expression vector and ligated mixtures were transformed into competent cells of *Escherichia coli* $DH_5\alpha$ by electroporation. The same condition was used for cloning of the *f-PLAC1* in *Nco*I/*Hind*III restriction sites of digested/dephosphorylated pET-32a resulting in a fusion sequence containing Thioredoxin (Trx) at N-terminal and f-PLAC1 at C terminal (*Trx-PLAC1*). All constructs contained His_6-Tag at their 5′ end.

2.4. Sequencing

All sequencings were performed by an automatic sequencer

(MWG, Germany). pET32a (+) vector containing *Trx-PLAC1* was sequenced by T7 promoter and T7 terminator universal primers. pCold-F and pCold-R primers were employed for sequencing of pColdI vector containing *f-PLAC1* and *t-PLAC1*.

2.5. Recombinant protein expression

2.5.1. Small-scale expression of recombinant proteins

All constructs were sequenced and the results confirmed that there was no alteration or base substitution in the sequence of the cloned products. Constructs containing the genes of interest were transformed to five *Escherichia coli* strains, *BL21 (DE3), Origami™ (DE3), Rosetta2 (DE3), Rosettagami (DE3)* pLysS, *and Shuffle T7 (DE3)* by electroporation. We followed the expression procedure described in the general pColdI vector manual. For small-scale expression, two milliliters (ml) of Terrific Broth (TB) medium containing 100 μg ml^{-1} Ampicillin for *BL21* (DE3), 100 μg ml^{-1} Ampicillin and 34 μg ml^{-1} chloramphenicol for *Rosetta2* (DE3), 100 μg ml^{-1} Ampicillin, 34 μg ml^{-1} chloramphenicol and 15 μg ml^{-1}kanamycin for *Rosettagami* (DE3) pLysS strain, 100 μg ml^{-1} Ampicillin, 15 μg ml^{-1} kanamycin and 12.5 μg ml^{-1} tetracycline for *Origami* (DE3) or 100 μg ml^{-1}Ampicillin for *Shuffle T7 (DE3)*, was inoculated with a fresh bacterial colony harboring the expression plasmid and grown at 37 °C overnight. Then 10 ml of fresh medium was inoculated with 50 μl overnight cultures and grown at 37 °C with vigorous shaking (250 rpm) until the OD_{600} reached to 0.6 and 0.9. After induction with 0.1 and 1 mM IPTG, *E. coli* harboring pColdI plasmid cells were cultured at 15 °C for 24 h and those harboring pET32a were cultured at 22 °C for 12 h. The cells were harvested by centrifugation at 5000*g* for 15 min. The cell pellet was resuspended in a lysis buffer I (50 mM Tris-HCl, 500 mM NaCl, 10 mM imidazole, and 1 mM PMSF, pH 7.8). Then the cells were lysed by sonication on ice. The cell lysate was centrifuged at 12,000 g for 20 min at 4 °C, The samples of both insoluble (precipitation) and soluble fractions (supernatant) were placed on 12% sodium dodecyl sulfate-polyacrylamide (SDS-PAGE) gels, and protein bands were visualized by Coomassie Brilliant Blue staining after SDS-PAGE separation. For purification of f-PLAC1 and Trx-PLAC1 from inclusion body, different solubilization buffers for inclusion body aggregates were screened and purification protocol was optimized. In brief, cells harvested from 200 ml culture were lysed in a lysis buffer II (50 mM Tris-HCl, 5 mM EDTA, 1 mM PMSF, pH 8.5) and sonicated for 10 cycles of 1 min each (short pulses of 20 s followed by a gap of 40 s). Cell lysate was centrifuged at 20,000 × g for 20 min at 4 °C. Then the pellet was suspended in wash buffer I (50 mM Tris-HCl, 5 mM EDTA, 1 mM PMSF, and 0.5% deoxycholic acid (DOC), pH 8.5) followed by sonication and centrifugation as mentioned above. Then, the pellet was aliquated to six fractions and solubilized in six different solubilization buffers for 1 h at room temperature: A: (50 mM Tris-HCl, 5 mM EDTA, 1 mM PMSF, and 8 M urea, pH 8.5), B: (50 mM Tris-HCl, 5 mM EDTA, 1 mM PMSF, and 6 M GdnHCl, pH 8.5), C: (50 mM Tris-HCl, 5 mM EDTA, 1 mM PMSF, and 2 M urea, pH 12), D: (50 mM Tris-HCl, 5% glycerol, 0.1 mM EDTA, 50 mM NaCl, and 0.4% Triton X-100, pH 7.9) [28], E: (50 mM Tris-HCl, 5 mM EDTA, 1 mM PMSF, 6 M n -propanol, and 2 M urea, pH 8.5), and F: (50 mM Tris-HCl, 5 mM EDTA, 1 mM PMSF, 6 M β-mercaptoethanol, and 2 M urea, pH 8.5) [29]. To determine the optimal conditions for the solubilization of inclusion bodies, samples of both insoluble (precipitation) and soluble fractions (supernatant) were placed on 12% SDS-PAGE gels, and protein bands were visualized by Coomassie Brilliant Blue staining. Based on results, wash buffer I and solubilization buffer C were selected for purification of Trx-PLAC1 and f-PLAC1, respectively.

2.5.2. Large-scale production and purification

Large-scale expression of f-PLAC1, t-PLAC1 and Trx-PLAC1 were carried out in the *Origami™* (DE3) strain. Pre-culture was performed for 16 h in 5 ml TB medium at 37 °C; the culture was then diluted with 400 ml TB supplemented with 100 μg ml^{-1} Ampicillin and 15 μg ml^{-1} kanamycin. When OD_{600} reached 0.6, cold shock (37 °C–15 °C) was initiated and expression was induced with 0.1 mM IPTG. Cells were further cultured for 24 h at 15 °C. The induced cells were harvested by centrifugation at 5000*g* for 15 min. The cell pellet was resuspended in lysis buffer I and lysed by sonication on ice. Following centrifugation at 12,000*g* for 20 min at 4 °C, supernatant was collected and applied to Ni Sepharose column (GE Healthcare). His_6-tagged recombinant t-PLAC1 was purified using the immobilized metal affinity chromatography (IMAC) as described by the manufacturer on native condition; in brief washing the column was done with wash buffer II (50 mM Tris-HCl, 500 mM NaCl, 20–50 mM imidazole, and 1 mM PMSF, pH 7.8), then elution with elution buffer (50 mM Tris-HCl, 500 mM NaCl, 250 mM imidazole, and 1 mM PMSF, pH 7.8) was carried out. Finally, glycerol (10% v/v) was added to the eluted samples and stored at −20 °C. For purification of Trx-PLAC1, two times of sonication were done, the first one was after addition of lysis buffer I and the second was after addition of wash buffer I. The rest of purification method was similar to t-PLAC1 whish was mentioned above. The purity and molecular weight of the fractions containing purified t-PLAC1 proteins was determined by SDS-PAGE gel electrophoresis under reducing condition. For on-column refolding of f-PLAC1, pellet solubilized in buffer C for 1 h at room temperature with mild shaking 1500 rpm, was centrifuged at 10,000*g* for 15 min. The supernatant fraction was collected and then loaded on a 1.5 ml Ni sepharose™ high performance (GE healthcare, United Kingdom). Refolding of the bound protein is performed using a linear gradient from 2 to 0 M of urea, and in 0 M urea, we decreased the pH from 12 to 7.8. A gradient volume of 30 ml and a flow rate of 0.5 ml min^{-1} were applied. Column was washed with 5 ml of buffer without urea and pH 7.8 after the gradient has come to its endpoint. Following that, the flow-through was collected and loaded onto a Superdex 75 Prep Grade (GE Healthcare life sciences) column and eluted with buffer I (20 mM Tris–HCl pH 8.0, 150 mM NaCl). The purity of the recombinant protein was confirmed by SDS–PAGE and DLS analyses.

2.5.3. Protein analysis and yield calculation

The expression of recombinant PLAC1 (t-PLAC1, f-PLAC1 and Trx-PLAC1) were analyzed on a 12% SDS-PAGE gel stained with coomassie brilliant blue R-250 (Bio-Rad). The protein concentration was determined by the Bradford protein assay method using BSA as the standard [30,31] or by spectroscopy using a calculated molar absorption coefficient at 280 nm (e280) of 24,575, 12,865 and 38,680 $M^{-1}cm^{-1}$ for the purified protein f-PLAC1, t-PLAC1 and Trx-PLAC1 respectively. The percentage of solubilization were also measured based on the turbidity of the solution at 350 nm [32].

2.6. Densitometric analysis and molecular weight determination

DLS uses scattered light to measure the rate of protein particles diffusion. The obtained motion data are processed to derive a size distribution for the sample, where the size is given by the hydrodynamic radius of the protein particle. The hydrodynamic size depends on both mass and shape of the molecules. Densitometric analysis and molecular weight determination of purified PLAC1 molecules were performed according to the protocol published elsewhere [33]. For densitometric analysis, SDS-PAGE gels were scanned and density of specific bands of recombinant proteins was analyzed using the program AlphaEase FC Software (Version 5.0.1)

with standard settings calculating AUC (area under curve) for each band. The sum of the band densities in lane was set to 100% and relative percentage of each band was calculated accordingly.

2.7. The use of dynamic light scattering (DLS) to characterize protein aggregation

Recombinant proteins were dialyzed against PBS buffer (0.15 M, pH 7.8) at 4 °C, overnight. Then the average size and size distribution of the recombinant proteins were determined by dynamic light scattering by photon correlation spectroscopy. A Zetasizer Nano ZS instrument (Malvern Instruments, UK) was used to measure particle size at 25 °C. Prior to loading in the cuvette, the solutions were filtered through 0.22 μm Millipore filters [34,35].

2.8. Disulfide bridge determination

Thiol titration was carried out according to the manufacturer's instruction. In brief 25 μl of recombinant protein was mixed with 250 μl of 100 mM sodium phosphate (pH 8.0) and 1 mM EDTA with or without 50 mM dithiothreitol (DTT) and 6 M Gu.HCl buffer containing 5 μl of 4 mg ml^{-1} of DTNB for 15 min at room temperature. The absorbance was measured at 412 nm with a molar absorbance value of 14,150 M^{-1} cm^{-1} for PBS and 13,880 for Gu.HCl buffer. In the case of reduced protein, dialysis was done against PBS-EDTA solution to remove DTT [36–38].

2.9. Production of polyclonal antibodies against human PLAC1

Two PLAC1-specific Rabbit polyclonal antibodies [4,39], were produced. According to the published amino acid sequence, two synthetic peptides; $PLAC1^{166-177}$ (CVFSEEEHTQVP) [11,39] and $PLAC1^{117-127}$ (APQKSPWLTKP) [4] corresponding to extracellular segment of human PLAC1 were conjugated separately with Imject Maleimide-activated mcKeyhole Limpet Hemocyanin (Thermo Scientific, Rockford, IL, USA) and injected to New Zealand White Rabbits. Antibody purification was performed using peptide-coupled affinity column after five immunizations. The purity of antibodies was assessed by SDS-PAGE.

2.10. Western blotting

After separation on SDS-PAGE gel, proteins were transferred to nitrocellulose membranes (Hybond-ECL; Amersham) in 100 mM Tris-HCl pH 7.5, containing 2.5 M NaCl, 0.5% Tween 20, 2% Triton X-100 and 20% (v/v) methanol, for 1 h at 1 mA/cm^2, using a Bio-Rad apparatus (Berkeley, California). To detect proteins, membranes blocked in BSA 5% for 16 h then incubated for 1 h at 4 °C either with a horseradish peroxidase (HRP)-conjugated monoclonal anti-His antibody (Roche) at a 1:100,000 dilution or with a polyclonal rabbit anti-PLAC1 antibody at a concentration of (50 ng ml^{-1}) [4,11,39]. In the latter case, membranes were washed and incubated for 1.5 h at room temperature with the corresponding secondary antibodies, HRP-conjugated sheep anti-rabbit (Sina Biotech, Tehran, Iran) at a 1:3000 dilution. Membranes were developed with ECL detection kit according to the manufacturer's instruction (Pierce).

2.11. Indirect ELISA

An indirect ELISA was set up for detection of full length and truncated human PLAC1 using PLAC1-specific polyclonal antibodies. In brief, plates were coated with 10 μg ml^{-1} recombinant proteins for 1.5 h at 37 °C. Plates were washed with PBS-Tween and blocked with PBS-BSA 2.5% overnight. Titrating concentrations of purified PLAC1-specific polyclonal antibodies were added to the wells and incubation was continued for 1.5 h. Signals were developed after sequential addition of HRP-conjugated sheep anti-rabbit Ig (Sina Biotech, Tehran, Iran) and TMB as chromogen. Optical density (OD) of the wells was measured at 450 nm.

2.12. Circular dichroism (CD) measurements

Full-length recombinant protein (f-PLAC1) was dialyzed against 50 mM Tris buffer (pH 7.8) at 4 °C, overnight. Far-UV CD spectra were recorded on a JASCO J-715 spectropolarimeter (Japan), using protein solutions of 0.2 mg ml^{-1} in 50 mM Tris buffer (pH 7.8) by 1 mm cell. Background signals were corrected against buffer blank and all spectra were collected from 200 to 260 nm. Data was presented in terms of molar ellipticity [ɵ] (deg cm^2 $dmol^{-1}$), based on the mean amino acid residual weight (MRW) of 110 Da. The molar ellipticity was determined as $[ɵ] = (ɵ \times 100\ MRW)/(cl)$, where c is the protein concentration in mg ml^{-1}, l is the light path length in centimeters, and ɵ is the measured ellipticity in degrees at wavelength λ. Noise of data was smoothed using JASCO J-715 software, including the fast Fourier-transform noise reduction routine, which allows enhancement of signal to noise ratio [37,40]. After normalization of CD spectra against protein concentration, normalized spectra were deconvoluted by the use of CDSSTR algorithm and Reference set 7 at Dichroweb [41,42]. Finally total helix and sheets were obtained.

2.13. Bioinformatics analysis: protein 3D structure prediction with I-TASSER server

Three-dimensional model of PLAC1 was generated through multiple threading alignments by LOMETS and iterative TASSER simulations [43,44]. I-TASSER generates full-length model of proteins by excising continuous fragments from threading alignments and then reassembling them using replica-exchanged Monte Carlo simulations. I-TASSER is a hierarchical protein structure modeling approach based on the secondary-structure enhanced Profile-Profile threading Alignment (PPA) [45] and the iterative implementation of the Threading ASSEmbly Refinement (TASSER) program [46]. The detail of the ITASSER method has been described in Refs. [47,48]. The two parameters evaluating the quality and accuracy of the model are defined as C-score and TM-score, respectively. C-score is a confidence score for estimating the quality of predicted models by I-TASSER. C-score typically ranges from −5 to +2, where a C-score of higher value signifies a model with a high confidence and vice-versa. A TM-score >0.5 indicates a model of correct topology and a TM-score <0.17 means a random similarity.

3. Results

3.1. Construction of the expression system and preliminary protein production

The expression of human genes in *E. coli* may suffer from low yields due to exhibiting distinct codon usage and the lack of the suitable environment for proper folding. To overcome these issues, different plasmids and strains of *E. coli* were used to express PLAC1. The sequence encoding amino acids 117–212 (t-PLAC1) was cloned into pColdI and that encoding 23–212 (f-PLAC1) was cloned into pET-32a and pColdI vectors. The constructs were transformed into several *E. coli* strains, including *Origami* ™ (DE3), *Shuffle T7* (DE3), *BL21* (DE3) and *Origami2* (DE3) and induced for protein expression. Then, the protein expression was evaluated by the SDS-PAGE and Western blot analyses (Fig. 1A and B).

The optimum expression level of t-PLAC1 was obtained in the presence of 1 mM IPTG ($OD_{600nm} = 0.9$) after 24 h induction at 15 °C

(A)

Truncated-PLAC1 (PLAC1$^{117-212}$)								
pcoldI+PLAC1 OD:0.6				Marker	pcoldI+PLAC1 OD:0.9			
IPTG 0.1	IPTG 0.1	IPTG 1	IPTG 1		IPTG 0.1	IPTG 0.1	IPTG 1	IPTG 1
soluble	insoluble	soluble	insoluble		soluble	insoluble	soluble	insoluble

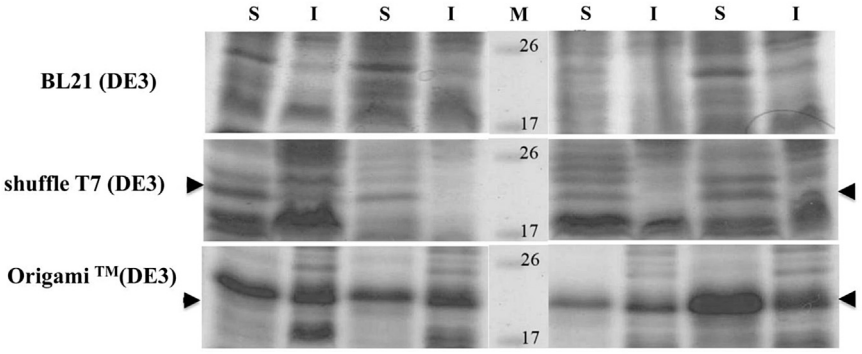

(B)

pcoldI+PLAC1 OD:0.6 *BL*21(DE3)		Marker	pcoldI+PLAC1 OD:0.9 *Origami*^{TM}(DE3)		pcoldI+PLAC1 OD:0.9 *Shuffle T7* (DE3)	
IPTG 0.1	IPTG 0.1		IPTG 1	IPTG 1	IPTG 1	IPTG 1
soluble	insoluble		soluble	insoluble	soluble	insoluble

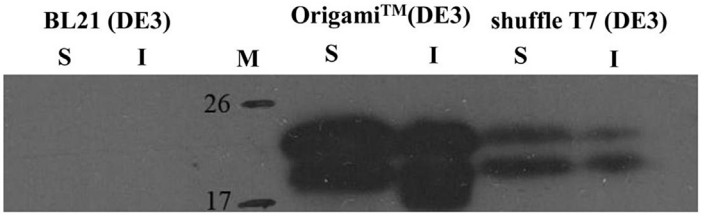

Fig. 1. SDS-PAGE of recombinant PLAC1.
(A) Expression and (B) Western blot analysis (using anti-His tag antibody) of t-PLAC1 in different strains of *E. coli*.
(C) Expression and (D) Western blot analysis (using anti-His tag antibody) of f-PLAC1 in different strains of *E. coli*.
(E) Expression and (F) Western blot analysis (using anti-His tag antibody) of Trx-PLAC1 in different strains of *E. coli*.
50 μg of protein concentrations were run in parallel with molecular mass standards on a 12% gel and stained with Coomassie Blue R-250.
(S = soluble fraction and I = insoluble fraction).

in *Origami*™ (DE3). Under this condition, the soluble PLAC1 was about half the total expressed protein. *Shuffle T7* (DE3) also yielded a considerable amount of protein, albeit with lower efficacy. No soluble protein was detected when *BL21* (DE3) was used.

f-PLAC1 was over-expressed as either alone (f-PLAC1) or as a fusion protein with thioredoxin (Trx-PLAC1). The highest levels of protein expression for f-PLAC1 and Trx-PLAC1 were obtained in *E. coli Rosetta*2 (DE3) cells (Fig. 1C–F). The results indicated that f-PLAC1 was expressed as inclusion bodies (IBs) in all tested strains, while the main part of Trx-PLAC1 were expressed as soluble forms in *BL21* (DE3), *Rosetta*2 (DE3), *Rosetta-gami* (DE3) pLysS and *shuffle T7* (DE3).

3.2. Solubilization of IBs

Various buffers were tested to find the best condition for the solubilization of IBs. The results indicated that the highest level of soluble protein was present in buffer C containing Urea 2 M, (pH = 12). A high level of the soluble form of f-PLAC1 was also obtained in buffer A (Urea 8 M, pH = 8). In the case of fusion-PLAC1 (Trx-PLAC1), the recombinant protein was completely solubilized in wash buffer I, containing a mild detergent (0.5% of deoxycholic acid) prior to solubilization in solubilization buffers (Fig. 2A and B). Moreover, the solubilized PLAC1 was filtered and its solubility measured by considering OD_{450} nm (data not shown). The results

(C)

Full-PLAC1 (PLAC1$^{23\text{-}212}$)								
pcoldI+PLAC1 OD:0.6				Marker	pcoldI+PLAC1 OD:0.9			
IPTG 0.1	IPTG 0.1	IPTG 1	IPTG 1		IPTG 0.1	IPTG 0.1	IPTG 1	IPTG 1
soluble	insoluble	soluble	insoluble		soluble	insoluble	soluble	insoluble

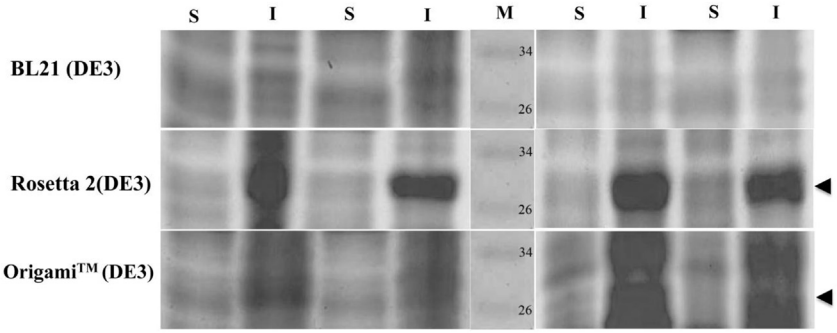

(D)

pcoldI+PLAC1 OD:0.9 *BL*21(DE3)		pcoldI+PLAC1 OD:0.6 *Origami*^{TM}(DE3)		pcoldI+PLAC1 OD:0.9 *Rosetta*2(DE3)		Marker
IPTG 0.1	IPTG 0.1	IPTG 0.1	IPTG 0.1	IPTG 0.1	IPTG 0.1	
soluble	insoluble	soluble	insoluble	soluble	insoluble	

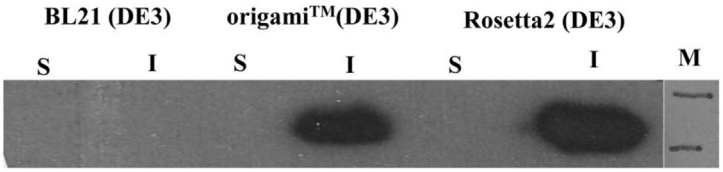

Fig. 1. (*continued*).

indicated a homogenate soluble PLAC1, which was useful for further studies.

3.3. Purification of expressed proteins

The purification of recombinant proteins t-PLAC1 and f-PLAC1 was done by affinity chromatography. The flow-through from f-PLAC1 and trx-PLAC1 (Fig. 3B) were further loaded onto a gel filtration column to remove further contaminants, aggregated protein and small molecular weight impurities (Fig. 3C). The purified proteins had more than 95% purity, as detected by SDS-PAGE. While t-PLAC1 showed two bands of about 18 and 22 KD, f-PLAC1 and Trx-PLAC1 indicated bands of 27.2 and 45 KD respectively after on-column refolding of proteins (Fig. 3 and Fig. S2). Moreover, the results demonstrated an intense band corresponding to the estimated molecular weight of PLAC1, as detected by Western blot using commercial anti His-tag antibody and specific polyclonal antibodies [39]. Indeed, PLAC1-specific polyclonal antibodies directed against peptides 117–127 and 166–177 showed parallel pattern of reactivities with t-PLAC1 (Fig. 4A) or f-PLAC1 (Fig. 4B) as determined by indirect ELISA. Reactivity with t-PLAC1 was more pronounced giving an optical density above 2 with as low as 325 ng ml^{-1} antibody. These results suggested a reasonable folding of purified recombinant proteins. Based on Bradford assay and spectroscopy results, approximately 35 mg of purified f-PLAC1 was obtained from 1 L of medium after on-column refolding. While the yield of t-PLAC1 and Trx-PLAC1 were 10 and 25 mg L^{-1} of purified protein after native purification of proteins, respectively.

3.4. DLS analysis

DLS is very useful to detect small amounts of aggregated proteins. The main components (100%) of f-PLAC1 (Fig. 5A and B) and Trx-PLAC1 (Fig. 5C and D) represent 3.76 and 61.43 nm in size after IMAC chromatography, while their correlated size were changed to 1.86 and 9.78 nm after gel filtration chromatography respectively. No part of aggregates was observed as determined by DLS. Our results clearly showed the polydispersity percentage of the purified proteins were 18 which were less than 20% indicating monodispersity of obtained proteins (see Table 2).

3.5. Estimation of disulfide bridges

Recombinant PLAC1 was expressed in the *Origami* (DE3) and *Shuffle T7* strains for appropriate formation of disulfide bridges. Incubation of PLAC1 with DTNB (Ellman reagent) showed that some

(E)

Fusion-PLAC1 (Trx-PLAC1)								
pET32a+PLAC1 OD:0.6				Marker	pET32a +PLAC1 OD:0.9			
IPTG 0.1	IPTG 0.1	IPTG 1	IPTG 1		IPTG 0.1	IPTG 0.1	IPTG 1	IPTG 1
insoluble	soluble	insoluble	soluble		soluble	insoluble	soluble	insoluble

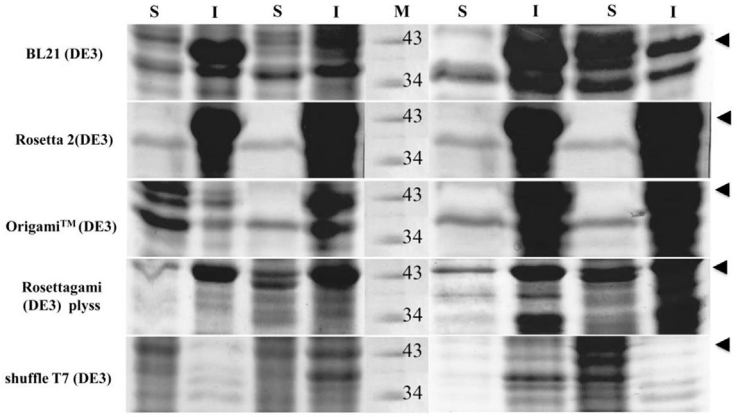

(F)

pET32a+PLAC1$^{23-212}$ OD:0.6 *Origami*^{TM}(DE3)		pET32a+PLAC1$^{23-212}$ OD:0.9 *Rosetta*2(DE3)		pET32a+PLAC1$^{23-212}$ OD:0.9 *Rosettagami* (DE3) pLysS		pET32a+PLAC1$^{23-212}$ OD:0.9 *Shuffle T7* (DE3)		Marker	pEt32a+PLAC1$^{23-212}$ OD:0.6 *BL*21(DE3)	
IPTG 0.1	IPTG 0.1	IPTG 1	IPTG 1	IPTG 0.1	IPTG 0.1	IPTG 0.1	IPTG 0.1		IPTG 0.1	IPTG 0.1
soluble	insoluble	soluble	insoluble	soluble	insoluble	soluble	insoluble		insoluble	soluble

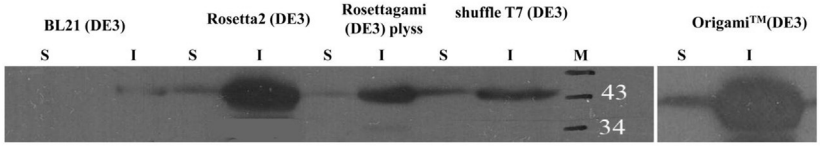

Fig. 1. (*continued*).

cysteines were buried inside the non-accessible area of PLAC1. f-PLAC1 was treated with denaturant agent Gu.HCl. Incubation of the recombinant PLAC1 with DTNB (Ellman reagent) is shown in (Table 1). The results clearly demonstrated that four Cys residues were involved in the disulfide bridges, whereas the remaining free thiol groups reacted with DTNB. At the same time, the DTNB assay under denaturing and reducing conditions (with DTT) caused an increase in the release of TNB, confirming the formation of disulfide bonds in the absence of a reducing agent. These results are in line with the study by Jovine *et al*, showing that PLAC1 contained two disulfide bridges in the ZP domain [5,49].

3.6. CD spectra of full-PLAC1

The far-UV CD full length of PLAC1 spectrum is shown in Fig. 6. The secondary structure of f-PLAC1 consisted of 11.2% α-helix; 53% of β-sheet + turn; and 35.8% of random structures as considered by JASCO J-715 software. The results were found to be in accordance with the predicted secondary structure of PLAC1 based on the primary sequence of the molecule obtained from the *PSIPRED* protein structure prediction server (Fig. S3). The soluble form of PLAC1 exhibited a considerable amount of secondary structure as determined by the CD spectra.

3.7. Homology modeling of PLAC1

The capability of i-TASSER in predicting protein structure was demonstrated by Yang J. *et al* [50]. A model of f-PLAC1 was built using the I-TASSER program which automatically generated high quality predictions of the 3D structure of protein molecules from their amino acid sequences [44]. The C-score, which is a confidence score for estimating the quality of predicted models by I-TASSER and typically is from −5 to 2, high value indicating a model with high confidence [51], was 0.94 for PLAC1. The TM-score of PLAC1, a parameter for measuring the quality of the modeling prediction [51] was found to be 0.60 ± 0.14, indicating a high modeling

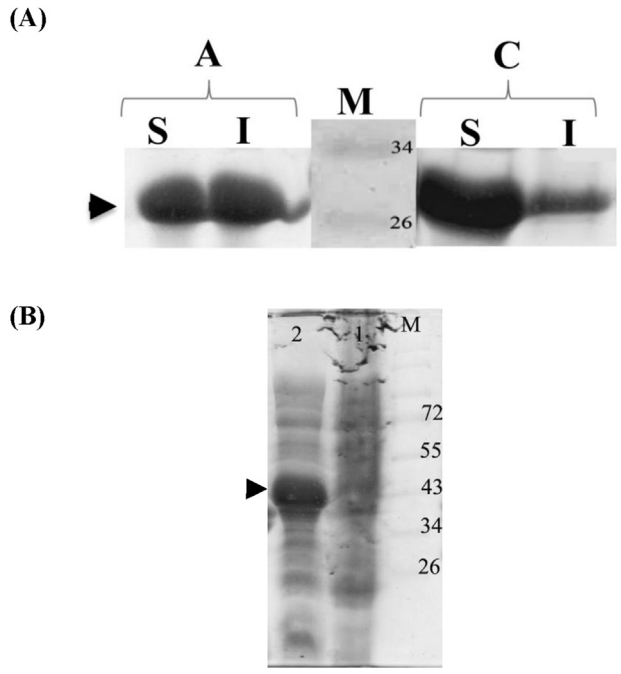

Fig. 2. (A) SDS-PAGE of selected solubilization buffers for f-PLAC1 protein expressed in *Rosetta*2 (DE3). (S = soluble fraction and I = insoluble fraction). (B) Solubilization of Trx-PLAC1.

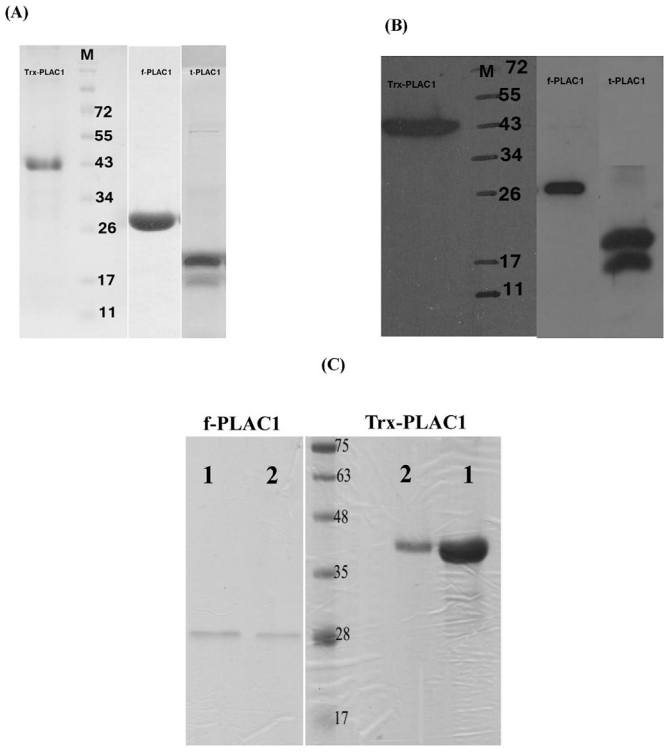

Fig. 3. (A) SDS-PAGE and (B) Western blot analysis (using specific polyclonal antibody) of purified recombinant PLAC1. (C) SDS-PAGE analysis after 1) IMAC and 2) Gel filtration chromatography.

accuracy. A TM-score >0.5 also indicates a model of correct topology. ZP3 conserved domain was detected, while, four cysteines Cys^{30}-Cys^{115} and Cys^{61}-Cys^{80} could generate two disulfide bridges as predicted in the model. The other cysteines (C^{49}, C^{128}, C^{146}, C^{161}, C^{163}, C^{166} and C^{178}) were free and not involved in disulfide bridges (Fig. 7).

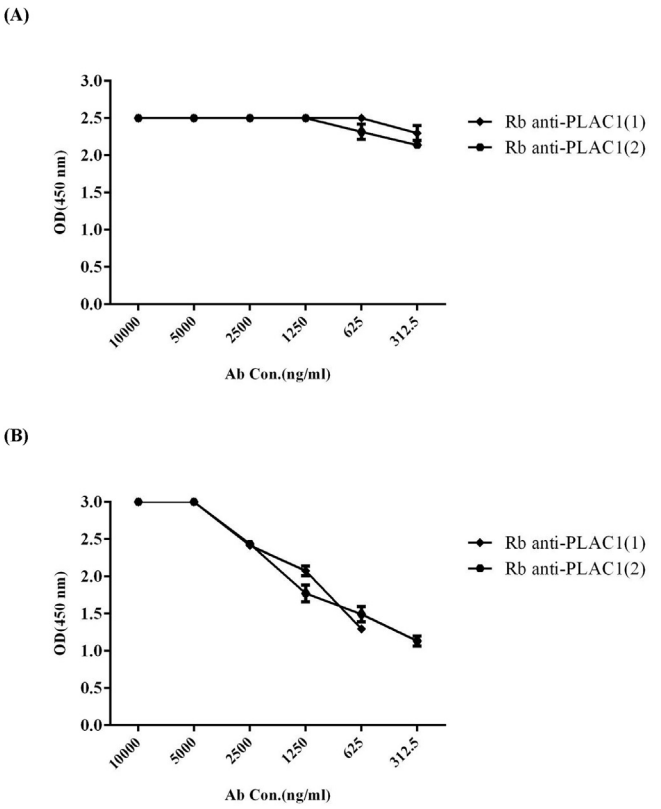

Fig. 4. Titration of anti-PLAC1 antibody in immunized mouse serum by indirect ELISA. Hyperimmunized serum was serially titrated on a (A) recombinant t-PLAC1 and (B) f-PLAC1 coated plate. aldrich). All experiments are repeated at least 3 times, the error associated with each point falls within 5% of the value.

4. Discussion

PLAC1 is a newly-identified cancer testis antigen with widespread expression in cancer tissues and cells [4,6,8–11]. Nevertheless, limited data are available on the efficient production of this biomolecule or its structure. Chemically synthesized proteins are costly and usually hard to obtain. Hence, it is proposed to employ an expression host that is more cost-effective and provides a sufficient amount of the biomolecule. The purpose of the current study was to establish and optimize the expression and purification procedure for recombinant PLAC1 using different *E. coli* strains and to characterize secondary structure of the purified protein.

PLAC1 is a membrane-associated protein. This protein, containing a large number of cysteine residues. Owing to the fact that the protein is located at the cell surface, it is probable that some of these cysteines may be involved in disulfide bond formation as predicted by the i-TASSER program. Here, three recombinant PLAC1 proteins were produced by employing two different strategies based on the predicted topology of PLAC1 protein (Scheme 2, supplementary data) that included: 1) Application of low temperature for optimization of recombinant protein production using the pCold vector containing the promoter of the cold shock-inducible gene for the major cold shock protein CspA, representing an improved expression level of the gene of interest following cold shock [17,52]. This vector also contains a lac operator downstream of the cspA promoter that regulates gene expression not only by

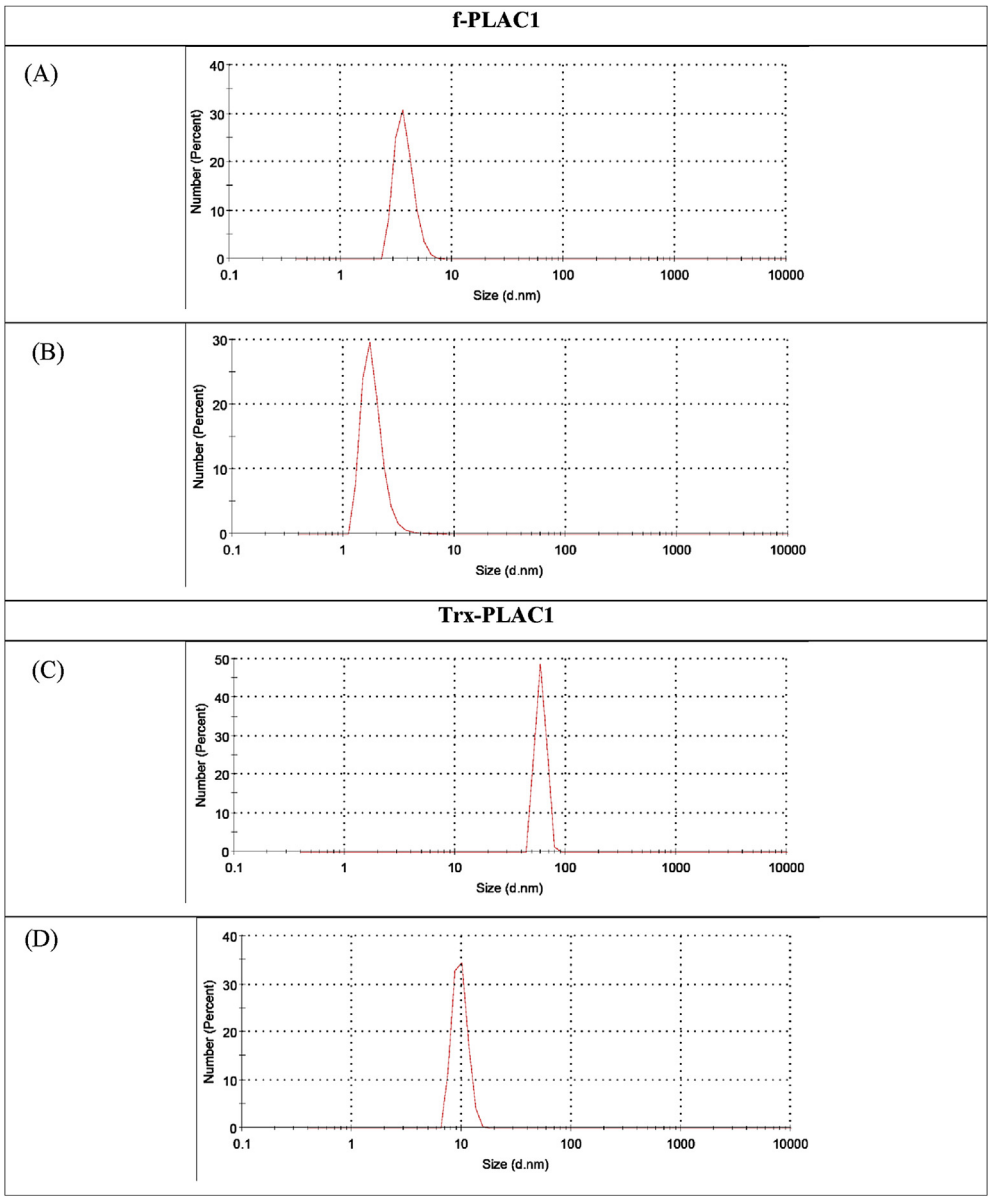

Fig. 5. Dynamic light scattering of (A), (B) f-PLAC1 and (C), (D) Trx-PLAC1. (A, C) are correlated to IMAC and (B, D) to gel filtration chromatography.

Table 1
Thiol content of recombinant PLAC1 was determined based on $OD_{412\ nm}$ upon treatment with and without DTT, Guanidine hydrochloride and Ellman reagent.

	Mol of SH per mol of protein − Gun-HCl		Mol of SH per mol of protein + Gun-HCl	
	-DTT	+DTT	-DTT	+DTT
f-PLAC1	3.67	9.32	6.9	11.01

temperature, but also by such lac stimulants as IPTG [17]. 2) The use of TRX tag partner; we clearly verified that the expression and solubility level of PLAC1 improved significantly when the protein was expressed as a fusion protein with TRX tag. Based on our results, the TRX tag was found to act as an excellent enhancer for production of PLAC1 in a soluble form (Fig. 1E). However, the exact mechanism by which TRX enhances the solubility of the protein

Table 2
DLS analysis of recombinant purified proteins.

Recombinant protein		f-PLAC1	Trx-PLAC1
IMAC	Size (nm)	3.76	61.43
	pdI	0.38	0.332
	pdI percentage	19%	25%
Gel filtration (superdex 75 prep)	Size (nm)	1.86	9.78
	pdI	0.3	0.3
	pdI percentage	18%	18%

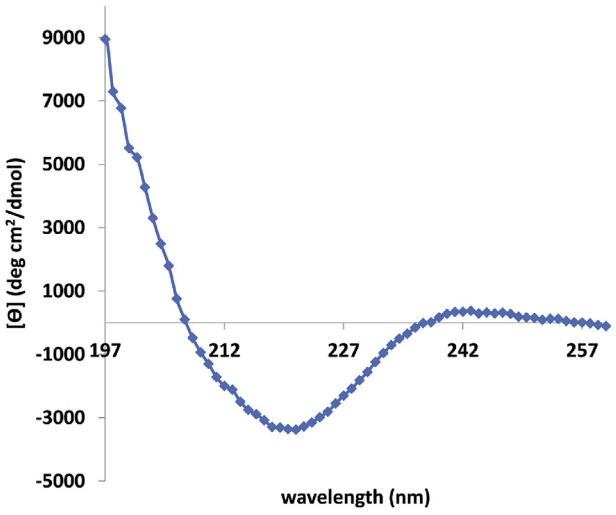

Fig. 6. Far-UV CD spectrum of native recombinant f-PLAC1. The concentration of protein was 0.2 mg ml^{-1} in Tris-HCl buffer (20 mM, pH 7.8). The spectrum was collected from 200 to 260 nm, and the background was corrected against buffer blank.

remains to be elucidated. Nonetheless, it has been reported that TRX may perform a passive rather than an active role in the folding of fusion passengers [32].

Several specialized host strains have been introduced to overcome the metabolic burden associated with a high level of protein expression. Cysteines in the *E. coli* cytoplasm are dynamically kept low by pathways associated with thioredoxin reductase and glutaredoxin. Therefore, a number of mutant strains have been introduced to conquer this problem such as the *Origami*, *Rosettagami* and *Shuffle T7*strains through the disruption of the *trx* and the genes encoding two reductases mutant (glutathione reductase and thioredoxin reductase), enhancing the formation of disulfide bonds in the *E. coli* cytoplasm. These strains in conjunction with *BL21* were employed for the production of recombinant proteins. In addition, the *Rosetta*2 strain was also used to overcome the codon usage barrier usually faced in the expression of human genes in *E. coli*. A high protein expression level of t-PLAC1 was achieved in the *Origami* ^{TM} (DE3) and *Shuffle T7* strains. It is conceivable that overexpression of disulfide-bond isomerase C (DsbC), a chaperone assisting the folding of proteins, in *Shuffle T7* (DE3) might help correct the formation of disulfide bonds and finally fold protein in a soluble form (Fig. 1). Moreover, t-PLAC1 showed two bands of about 18 and 22 KD. It may discuss that truncated protein with 18 kDa shows a different conformation of t-PLAC1 due to the disulfide bond remodeling. It has been reported that there are 11 cysteine residues in f-PLAC1. Their shuffling may form a different protein conformation. Therefore, it seems that the N-terminal portion (residues 23–117) of PLAC1 is important for the correct formation of a disulfide bridge in the nested protein during PLAC1 folding.

In the case of f-PLAC1, the highest level of protein expression was observed in the Rosetta2 (DE3) and OrigamiTM (DE3) strains although most of the protein was insoluble and present as inclusion bodies. During the expression of a recombinant protein in heterologous hosts, an elevated concentration of partially folded intermediates may have led to the aggregation of protein into IBs. In addition, the reducing state of bacterial cytoplasm, lack of chaperones, and posttranslational modifications may also contribute to formation of IBs [53,54]. Therefore, two different strategies have been implemented under specific conditions to decrease the

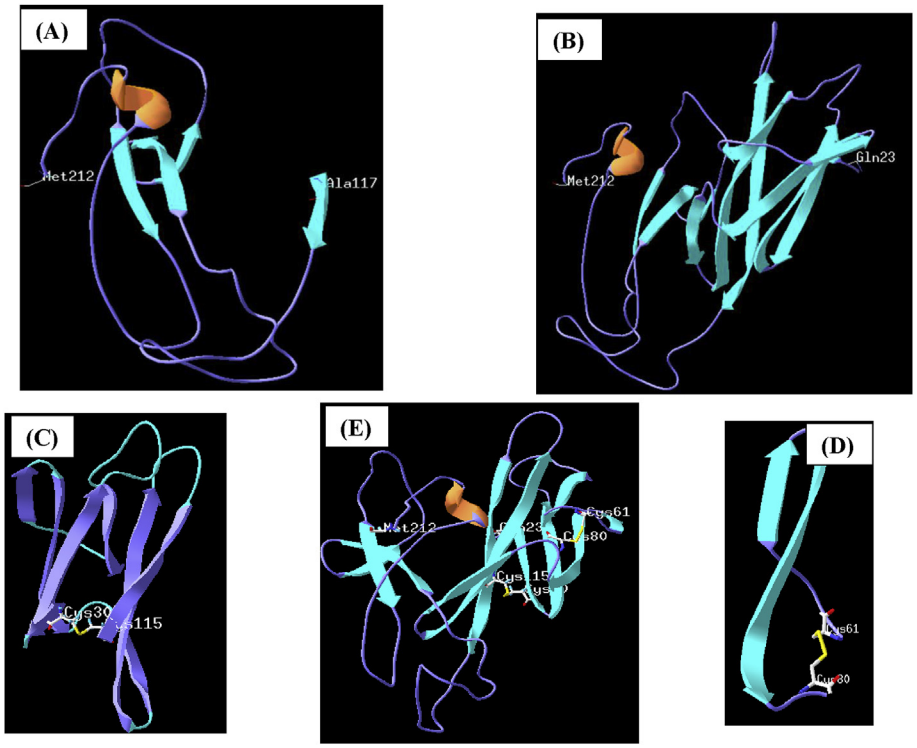

Fig. 7. 3D structure of predicted-PLAC1. (A) t-PLAC1, (B) F-PLAC1, (C) and (D) The location of two disulfide bridges. Cα and Cβ atoms are shown in white and disulfide bridges in yellow. E) The full structure of PLAC1 with disulfide bridges. The *de novo* structure of PLAC1 obtained from iTASSER server was used. (For interpretation of the references to colour in this figure legend, the reader is referred to the web version of this article.)

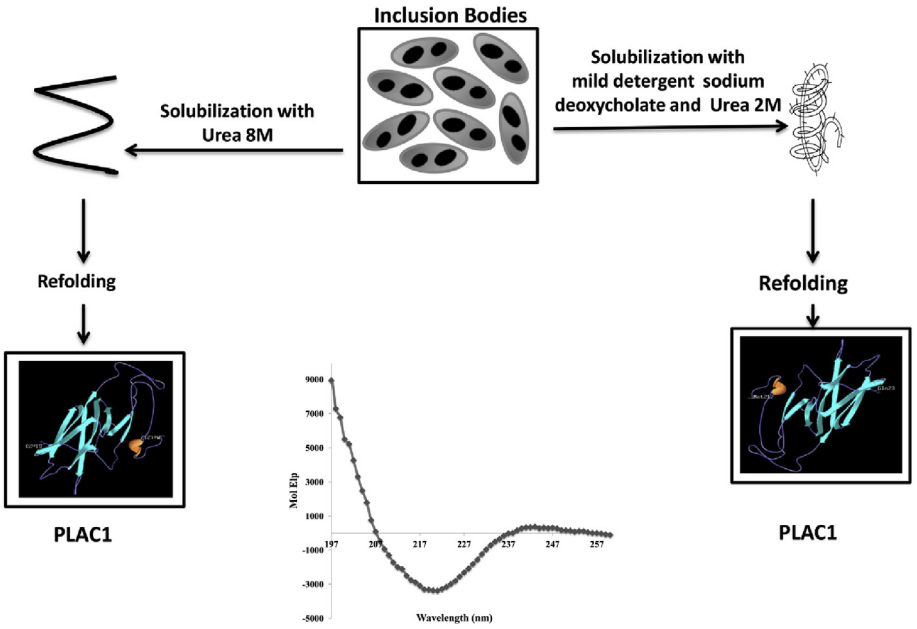

Scheme 1. The proposed model for inclusion bodies refolding.

formation of IBs. These include the use of cold shock and the fusion tag TRX system in which the culture temperature after the IPTG induction is lowered to 25 °C. Temperature variation is recognized to ease the production of active protein through a variety of mechanisms. Hydrophobic interactions, the main cause of IBs formation, have been reported to decrease if temperature is lowered [55–58]. Our result apparently showed that the cold shock system could not inhibit IBs formation whereas the use of TRX tag system could mostly avoid IBs formation leading to considerably lower amounts of proteins in IBs form. Thus, for those fractions of the protein which are expressed as IBs, solubilization and refolding are necessary.

Among the several steps needed to recover bioactive protein from IBs, the solubilization of IBs and the refolding of the solubilized protein are considered the most important [28,59]. Based on the CD spectrum, IBs represent native-like secondary structures. Solubilization of IBs in high concentrations of urea or GdnHCl may lead to a considerable loss of protein structure. On the other hand, mild solubilization agents (organic solvents, detergents like sodium deoxycholate (SDC), or high pH buffers) have been reported to maintain a part of the secondary and tertiary structures. In both cases, the refolding process can be optimized to recover properly folded native proteins. Mild solubilization of IBs can lead to lower protein aggregation in the refolding step. It has been reported that urea commonly has the ability to reduce hydrophobic interactions between water and protein molecules and facilitates solubilization of inclusion body associated proteins without disrupting their existing secondary structure.

In the current study, we demonstrated an increased solubility of the protein in the alkaline pH buffer containing 2 M urea, indicating the existence of both ionic and hydrophobic interactions in the inclusion bodies. The solubilization of the IBs protein with the maintenance of its native-like secondary structure has been reported to be a vital norm for its successful refolding into the native conformation. The advantages of pH-induced IBs solubilization have been demonstrated to be supported by the reversibility of pH-induced conformational conditions of comparable proteins such as the recombinant bovine growth hormone [60,61].

SDC, either alone or as a part of a sample lysis solution, has been applied to solubilize and extract plasma membrane proteins at low concentrations, [62–64]. Here, we were able to extract TRX-PLAC1 from IBs by SDC without using harsh chaotropic agents. The detergent probably interacts with the area of the protein that normally forms the interface with the membrane and, thus, acts as a substitute for the membrane associated protein (Fig. 2).

At the next step, we applied on-column refolding for the refolding of f-PLAC1 extracted from IBs (Fig. 3). Chromatography-assisted refolding offers several benefits including a higher concentration of the protein, simplifying the subsequent purification steps [65,66]. In addition, the use of this method has been shown to result in higher purity of renatured protein [67].

5. Conclusion

In this work, an efficient expression system for the human PLAC1 was developed. While being simple, this system provides an efficient method for the production of soluble PLAC1. Our results clearly showed the usefulness of the *cspA* promoter and fusion tag for the synthesis of recombinant PLAC1. Taken together, we were able to produce solubilized PLAC1 by employing two different methodologies and developed a procedure for the proper folding of PLAC1 as judged by circular dichroism. In line with an earlier report [29], we suggest that the use of a mild denaturant reagent such as SDC and a low concentration of chaotropic agent (Urea 2 M) can preserve some of the secondary and tertiary structures and improve the recovery of correctly folded native protein (Scheme 1).

Acknowledgements

This work was supported by a grant number 93/2446 from Avicenna Research Institute and (INSF) Iran National Science Foundation (No. 93041392).

Appendix A. Supplementary data

Supplementary data related to this article can be found at http://dx.doi.org/10.1016/j.pep.2017.03.011.

References

[1] M. Cocchia, R. Huber, S. Pantano, E.Y. Chen, P. Ma, A. Forabosco, M.S. Ko, D. Schlessinger, PLAC1, an Xq26 gene with placenta-specific expression, Genomics 68 (2000) 305–312.

[2] M. Fant, H. Barerra-Saldana, W. Dubinsky, B. Poindexter, R. Bick, The PLAC1 protein localizes to membranous compartments in the apical region of the syncytiotrophoblast, Mol. Reproduction Dev. 74 (2007) 922–929.

[3] M. Fant, A. Farina, R. Nagaraja, D. Schlessinger, PLAC1 (Placenta-specific 1): a novel, X-linked gene with roles in reproductive and cancer biology, Prenat. Diagn. 30 (2010) 497–502.

[4] M. Koslowski, U. Sahin, R. Mitnacht-Kraus, G. Seitz, C. Huber, Ö. Türeci, A placenta-specific gene ectopically activated in many human cancers is essentially involved in malignant cell processes, Cancer Res. 67 (2007) 9528–9534.

[5] L. Jovine, W.G. Janssen, E.S. Litscher, P.M. Wassarman, The PLAC1-homology region of the ZP domain is sufficient for protein polymerisation, BMC Biochem. 7 (2006) 11.

[6] W.A. Silva Jr., S. Gnjatic, E. Ritter, R. Chua, T. Cohen, M. Hsu, A.A. Jungbluth, N.K. Altorki, Y.-T. Chen, L.J. Old, PLAC1, a trophoblast-specific cell surface protein, is expressed in a range of human tumors and elicits spontaneous antibody responses, Cancer Immun. J. Acad. Cancer Immunol. 7 (2007) 18.

[7] X.Y. Dong, J.R. Peng, Y.J. Ye, H.S. Chen, L.J. Zhang, X.W. Pang, Y. Li, Y. Zhang, S. Wang, M.E. Fant, Plac1 is a tumor-specific antigen capable of eliciting spontaneous antibody responses in human cancer patients, Int. J. Cancer 122 (2008) 2038–2043.

[8] F.F. Liu, X.Y. Dong, X.W. Pang, Q. Xing, H.C. Wang, H.G. Zhang, Y. Li, Y.H. Yin, M. Fant, Y.J. Ye, The specific immune response to tumor antigen CP1 and its correlation with improved survival in colon cancer patients, Gastroenterology 134 (2008) 998–1006.

[9] J. Chen, X. Pang, F. Liu, X. Dong, H. Wang, S. Wang, Y. Zhang, W. Chen, PLAC1/CP1 gene expression and autologous humoral immunity in gastric cancer patients, Beijing da xue xue bao Yi xue ban 38 (2006) 124–127.

[10] L.J. Old, Cancer is a somatic cell pregnancy, Cancer Immun. J. Acad. Cancer Immunol. 7 (2007) 19.

[11] R. Ghods, M.-H. Ghahremani, Z. Madjd, M. Asgari, M. Abolhasani, S. Tavasoli, A.-R. Mahmoudi, M. Darzi, P. Pasalar, M. Jeddi-Tehrani, High placenta-specific 1/low prostate-specific antigen expression pattern in high-grade prostate adenocarcinoma, Cancer Immunol. Immunother. 63 (2014) 1319–1327.

[12] E.J. Devor, H.D. Reyes, D.A. Santillan, M.K. Santillan, C. Onukwugha, M.J. Goodheart, K.K. Leslie, Placenta-specific protein 1: a potential key to many oncofetal-placental OB/GYN research questions, Obstet. Gynecol. Int. 1 (2014) 678984–678989.

[13] J.-J. Lacapere, E. Pebay-Peyroula, J.-M. Neumann, C. Etchebest, Determining membrane protein structures: still a challenge!, Trends Biochem. Sci. 32 (2007) 259–270.

[14] G. Von Heijne, The membrane protein universe: what's out there and why bother? J. Intern. Med. 261 (2007) 543–557.

[15] K. McLuskey, A.W. Roszak, Y. Zhu, N.W. Isaacs, Crystal structures of all-alpha type membrane proteins, Eur. Biophys. J. 39 (2010) 723–755.

[16] S. Wagner, M.L. Bader, D. Drew, J.W. de Gier, Rationalizing membrane protein overexpression, TRENDS Biotechnol. 24 (2006) 364–371.

[17] H. Kobayashi, T. Yoshida, M. Inouye, Significant enhanced expression and solubility of human proteins in Escherichia coli by fusion with protein S from Myxococcus xanthus, Appl. Environ. Microbiol. 75 (2009) 5356–5362.

[18] A.M. Baca, W.G. Hol, Overcoming codon bias: a method for high-level overexpression of Plasmodium and other AT-rich parasite genes in Escherichia coli, Int. J. Parasitol. 30 (2000) 113–118.

[19] H.P. Sørensen, H.U. Sperling-Petersen, K.K. Mortensen, Production of recombinant thermostable proteins expressed in Escherichia coli: completion of protein synthesis is the bottleneck, J. Chromatogr. B 786 (2003) 207–214.

[20] D. Esposito, D.K. Chatterjee, Enhancement of soluble protein expression through the use of fusion tags, Curr. Opin. Biotechnol. 17 (2006) 353–358.

[21] W. Schumann, L.C.S. Ferreira, Production of recombinant proteins in Escherichia coli, Genet. Mol. Biol. 27 (2004) 442–453.

[22] H.P. Sørensen, K.K. Mortensen, Soluble expression of recombinant proteins in the cytoplasm of Escherichia coli, Microb. Cell Fact. 4 (2005) 1.

[23] J.A. Chesshyre, A.R. Hipkiss, Low temperatures stabilize interferon α-2 against proteolysis in Methylophilus methylotrophus and Escherichia coli, Appl. Microbiol. Biotechnol. 31 (1989) 158–162.

[24] M. Mujacic, K.W. Cooper, F. Baneyx, Cold-inducible cloning vectors for low-temperature protein expression in Escherichia coli: application to the production of a toxic and proteolytically sensitive fusion protein, Gene 238 (1999) 325–332.

[25] T. Makino, G. Skretas, G. Georgiou, Strain engineering for improved expression of recombinant proteins in bacteria, Microb. Cell Fact. 10 (2011) 30.

[26] P.H. Bessette, F. Åslund, J. Beckwith, G. Georgiou, Efficient folding of proteins with multiple disulfide bonds in the Escherichia coli cytoplasm, Proc. Natl. Acad. Sci. 96 (1999) 13703–13708.

[27] J. Lobstein, C.A. Emrich, C. Jeans, M. Faulkner, P. Riggs, M. Berkmen, SHuffle, a novel Escherichia coli protein expression strain capable of correctly folding disulfide bonded proteins in its cytoplasm, Microb. Cell Fact. 11 (2012), 56–56.

[28] R.R. Burgess, Refolding solubilized inclusion body proteins, Methods Enzym. 463 (2009) 259–282.

[29] A. Singh, V. Upadhyay, A.K. Panda, Solubilization and Refolding of Inclusion Body Proteins, Insoluble Proteins, Springer, 2015, pp. 283–291.

[30] M.M. Bradford, A rapid and sensitive method for the quantitation of microgram quantities of protein utilizing the principle of protein-dye binding, Anal. Biochem. 72 (1976) 248–254.

[31] M. Nazari, R. Emamzadeh, S. Hosseinkhani, L. Cevenini, E. Michelini, A. Roda, Renilla luciferase-labeled Annexin V: a new probe for detection of apoptotic cells, Analyst 137 (2012) 5062–5070.

[32] R. Khan, K. Rao, A. Eshwari, S. Totey, A. Panda, Solubilization of recombinant ovine growth hormone with retention of native-like secondary structure and its refolding from the inclusion bodies of Escherichia coli, Biotechnol. Prog. 14 (1998) 722–728.

[33] M.R. Nejadmoghaddam, M. Chamankhah, S. Zarei, A.H. Zarnani, Profiling and quantitative evaluation of three Nickel-Coated magnetic matrices for purification of recombinant proteins: helpful hints for the optimized nano-magnetisable matrix preparation, J. Nanobiotechnology 9 (2011) 1–11.

[34] W. Brown, Dynamic Light Scattering: the Method and Some Applications, Oxford University Press, USA, 1993.

[35] R. Cheraghi, M. Nazari, M. Alipour, A. Majidi, S. Hosseinkhani, Development of a targeted anti-HER2 scFv chimeric peptide for gene delivery into HER2-positive breast cancer cells, Int. J. Pharm. 515 (2016) 632–643.

[36] P.W. Riddles, R.L. Blakeley, B. Zerner, Ellman's reagent: 5, 5′-dithiobis (2-nitrobenzoic acid)—a reexamination, Anal. Biochem. 94 (1979) 75–81.

[37] M. Nazari, S. Hosseinkhani, L. Hassani, Step-wise addition of disulfide bridge in firefly luciferase controls color shift through a flexible loop: a thermodynamic perspective, Photochem. Photobiol. Sci. 12 (2013) 298–308.

[38] P.W. Riddles, R.L. Blakeley, B. Zerner, Reassessment of Ellman's reagent, Methods Enzym. 91 (1982) 49–60.

[39] R. Ghods, M.H. Ghahremani, M. Darzi, A.R. Mahmoudi, O. Yeganeh, A.A. Bayat, P. Pasalar, M. Jeddi-Tehrani, A.H. Zarnani, Immunohistochemical characterization of novel murine monoclonal antibodies against human placenta-specific 1, Biotechnol. Appl. Biochem. 61 (2014) 363–369.

[40] P. Manavalan, W.C. Johnson, Variable selection method improves the prediction of protein secondary structure from circular dichroism spectra, Anal. Biochem. 167 (1987) 76–85.

[41] A. Lobley, L. Whitmore, B. Wallace, DICHROWEB: an interactive website for the analysis of protein secondary structure from circular dichroism spectra, Bioinformatics 18 (2002) 211–212.

[42] L. Whitmore, B. Wallace, DICHROWEB, an online server for protein secondary structure analyses from circular dichroism spectroscopic data, Nucleic Acids Res. 32 (2004) W668–W673.

[43] A. Roy, A. Kucukural, Y. Zhang, I-TASSER: a unified platform for automated protein structure and function prediction, Nat. Protoc. 5 (2010) 725–738.

[44] Y. Zhang, I-TASSER server for protein 3D structure prediction, BMC Bioinforma. 9 (2008) 40.

[45] S. Wu, Y. Zhang, LOMETS: a local meta-threading-server for protein structure prediction, Nucleic Acids Res. 35 (2007) 3375–3382.

[46] Y. Zhang, J. Skolnick, Automated structure prediction of weakly homologous proteins on a genomic scale, Proc. Natl. Acad. Sci. U. S. A. 101 (2004) 7594–7599.

[47] S. Wu, J. Skolnick, Y. Zhang, Ab initio modeling of small proteins by iterative TASSER simulations, BMC Biol. 5 (2007) 17.

[48] Y. Zhang, Template-based modeling and free modeling by I-TASSER in CASP7, Proteins Struct. Funct. Bioinforma. 69 (2007) 108–117.

[49] N. Yonezawa, M. Nakano, Identification of the carboxyl termini of porcine zona pellucida glycoproteins ZPB and ZPC, Biochem. Biophys. Res. Commun. 307 (2003) 877–882.

[50] J. Yang, R. Yan, A. Roy, D. Xu, J. Poisson, Y. Zhang, The I-TASSER Suite: protein structure and function prediction, Nat. Methods 12 (2015) 7–8.

[51] Y. Zhang, J. Skolnick, Scoring function for automated assessment of protein structure template quality, Proteins Struct. Funct. Bioinforma. 68 (2007) 1020.

[52] G. Qing, L.-C. Ma, A. Khorchid, G. Swapna, T.K. Mal, M.M. Takayama, B. Xia, S. Phadtare, H. Ke, T. Acton, Cold-shock induced high-yield protein production in Escherichia coli, Nat. Biotechnol. 22 (2004) 877–882.

[53] S. Ventura, A. Villaverde, Protein quality in bacterial inclusion bodies, TRENDS Biotechnol. 24 (2006) 179–185.

[54] E. García-Fruitós, R. Sabate, N.S. de Groot, A. Villaverde, S. Ventura, Biological role of bacterial inclusion bodies: a model for amyloid aggregation, FEBS J. 278 (2011) 2419–2427.

[55] F.U. Hartl, J. Martin, Molecular chaperones in cellular protein folding, Curr. Opin. Struct. Biol. 5 (1995) 92–102.

[56] W.J. Welch, C.R. Brown, Influence of molecular and chemical chaperones on protein folding, Cell Stress Chaperones 1 (1996) 109.

[57] J.C. Young, V.R. Agashe, K. Siegers, F.U. Hartl, Pathways of chaperone-mediated protein folding in the cytosol, Nat. Rev. Mol. Cell Biol. 5 (2004) 781–791.

[58] N. Oganesyan, I. Ankoudinova, S.-H. Kim, R. Kim, Effect of osmotic stress and heat shock in recombinant protein overexpression and crystallization, Protein Expr. Purif. 52 (2007) 280–285.

[59] E.D.B. Clark, Protein refolding for industrial processes, Curr. Opin. Biotechnol. 12 (2001) 202–207.

[60] T.F. Holzman, J.J. Dougherty Jr., D.N. Brems, N.E. MacKenzie, pH-induced conformational states of bovine growth hormone, Biochemistry 29 (1990) 1255–1261.

[61] R. Khan, K. Rao, A. Eshwari, S. Totey, A. Panda, Solubilization of recombinant

ovine growth hormone with retention of native-like secondary structure and its refolding from the inclusion bodies of Escherichia coli, Biotechnol. Prog. 14 (1998) 722–728.
[62] M. Fountoulakis, R. Gasser, Proteomic analysis of the cell envelope fraction of Escherichia coli, Amino Acids 24 (2003) 19–41.
[63] C. Navarre, H. Degand, K.L. Bennett, J.S. Crawford, E. Mørtz, M. Boutry, Subproteomics: identification of plasma membrane proteins from the yeast Saccharomyces cerevisiae, Proteomics 2 (2002) 1706–1714.
[64] A. Helenius, E. Fries, H. Garoff, K. Simons, Solubilization of the Semliki Forest virus membrane with sodium deoxycholate, Biochim. Biophys. Acta (BBA)-Biomembr. 436 (1976) 319–334.
[65] X. Geng, L. Wang, Liquid chromatography of recombinant proteins and protein drugs, J. Chromatogr. B 866 (2008) 133–153.
[66] L. Wang, X. Geng, Protein renaturation with simultaneous purification by protein folding liquid chromatography: recent developments, Amino Acids 46 (2014) 153–165.
[67] E.J. Freydell, L.A. Van der Wielen, M.H. Eppink, M. Ottens, Size-exclusion chromatographic protein refolding: fundamentals, modeling and operation, J. Chromatogr. A 1217 (2010) 7723–7737.